Dependence of the ^{16}O + ^{16}O nuclear potential on nuclear incompressibility

S. Hossain,[1] A. S. B. Tariq,[2] Athoy Nilima,[2] M. Sujan Islam,[2] R. Majumder,[2] M. A. Sayed,[2] M. M. Billah,[2] M. M. B. Azad,[2] M. A. Uddin,[2] I. Reichstein,[3] F. B. Malik,[4,5,*] and A. K. Basak[2,†]

[1]*Department of Physics, Shahjalal University of Science and Technology, Sylhet 3114, Bangladesh*
[2]*Department of Physics, University of Rajshahi, Rajshahi 6205, Bangladesh*
[3]*School of Computer Science, Carleton University, Ottawa, Ontario K1S 5B6, Canada*
[4]*Department of Physics, Southern Illinois University, Carbondale, Illinois 62901, USA*
[5]*Department of Physics, Washington University, St. Louis, Missouri 63130, USA*

Nonmonotonic (NM) nucleus-nucleus potentials from the energy-density functional (EDF) theory including the Pauli principle have been considered for the nuclear incompressibility K in the range 188–266 MeV. The experimental cross sections of the ^{16}O + ^{16}O elastic scattering over the 31–350 MeV incident energies have been analyzed in the optical model using the NM potentials. Sensitivity of K on the elastic scattering data is studied and its value for infinite cold nuclear matter deduced to be 222 ± 5 MeV.

PACS number(s): 24.10.Ht, 25.70.Bc, 21.65.Mn

I. INTRODUCTION

The last two decades have witnessed considerable activity relating the nature of the nucleus-nucleus potential and the incompressibility of nuclear matter, K [1–3]. The latter is a poorly determined fundamental property of the equation of state (EOS) for cold nuclear matter [1] that can also shed light on neutron stars.

The widely used microscopic double-folding (DF) approach using the M3Y type of two-nucleon (NN) potentials [1,2,4] is found to be successful in describing the elastic and inelastic scattering processes including the refractive nuclear rainbows accompanying Airy interference. However, the DF potentials in the optical model (OM) fail to describe the opposite signs of vector analyzing powers (VAP) of the ^{6}Li and ^{7}Li elastic scattering by ^{58}Ni at $E_{\text{lab}} \approx 20$ MeV [5,6]. Moreover, DF potentials need large renormalization $N_R \approx$ 0.5–0.6 [4] in describing the ^{6,7}Li elastic scattering cross sections in the OM analyses. Furthermore, the inadequacy of DF potentials for not considering properly a repulsive core has been revealed in the successes following the addition of the latter to describe elastic scattering [7–11] and sub-barrier fusion [12–15] cross sections.

The isoscalar giant monopole resonance has been identified as a very sensitive probe to obtain information on the nuclear incompressibility K_A for nuclei of mass number A [16–24]. However, the deduction of K for infinite nuclear matter from the extracted K_A has been claimed to be model dependent [3,16–18,25].

The last 15 years have witnessed considerable successes of nonmonotonic (NM) α- and ^{6,7}Li-nucleus potentials [26,27, and references therein] derived from the energy-density functional (EDF) theory [28–30] and in the sudden approximation [31,32]. The most striking of them are:

(a) The EDF-derived NM potentials in OM have reproduced the opposite signs of VAP of ^{6}Li and ^{7}Li elastic

scattering by ^{58}Ni at $E_{\text{lab}} \approx 20$ MeV and by ^{120}Sn at 44 MeV in addition to their cross section data [27] without renormalization. However, binding energies (BEs) of the nuclei are to be reproduced well for good performance of EDF potentials [26,27].

(b) The NM α-^{90}Zr potentials in OM [26] are capable of reproducing the wide elastic scattering data including refractive Airy oscillations [4] by the potential in the nuclear interior over the energy interval of the 15.0–141.7 MeV remarkably well with χ-square per degree of freedom, χ^2, of single digits.

(c) α NM potentials have been found to be successful in reproducing the correct order of cross sections for one- [33], two- [34,35], and three-nucleon [36] stripping reactions on Si isotopes.

At higher projectile energies, the interaction time is small enough to justify the sudden approximation. At lower energies, the interaction is mainly at the surface and for the small overlaps, saturation density is not exceeded. Validity of the approximation is found, *a posteriori*, in the results reported over a diverse range of interactions and energies [26,27,33–36, and references therein].

The success of the NM potentials has been ascribed mainly to the microscopic consideration of the Pauli principle in the EDF theory of [28–30]. Pauli-distorted DF potential has been used in [37], where the resulting potential is shallow to account well for the ^{16}O + ^{16}O elastic scattering data at 124 and 145 MeV. Unphysical bound states of a nucleus in a monotonic deep potential are found to be removed in a phase equivalent NM shallow potential [38].

The ^{16}O nucleus is fairly compact and being spin-0 involves only central potentials. Its BE can be reproduced within $\approx 1.6\%$ with a simple density-distribution function (DDF) $\rho(r)$ of [39]. The boson symmetry effect in the ^{16}O + ^{16}O system is modulated by the mixture of diffractive and refractive structures, the latter becoming prominent at higher incident energies. Good quality data are available with Airy structures in the angular distributions of the ^{16}O + ^{16}O elastic scattering
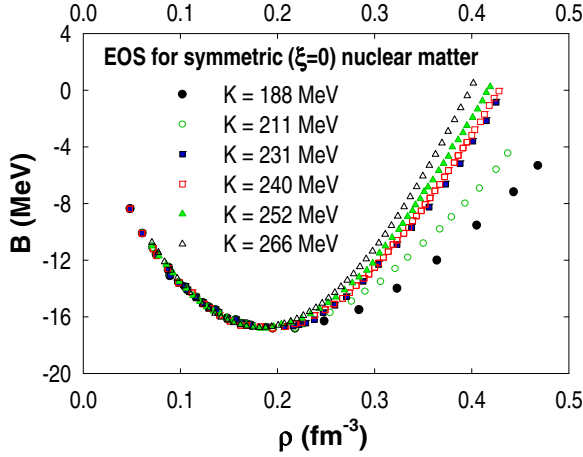

FIG. 1. (Color online) EOSs for six K values at the saturation point for symmetric infinite nuclear matter including the one from [28] with $K = 188$ MeV.

at energies beyond 60 MeV [40], making the system attractive to probe the interior potential for studying its K dependence.

II. FORMALISM

A. EDF theory

This work aims to report on how well the energy-independent EDF theory of Brueckner *et al.* (BCD) with the Pauli distortion can examine the sensitivity of the $^{16}\mathrm{O} + ^{16}\mathrm{O}$ elastic scattering data to K and deduce its value for infinite cold nuclear matter. In deriving the NM potentials, the Pauli-distorted EOS for infinite nuclear matter with non-Coulombic field is taken from [28]. The BE per nucleon $B(\rho, \xi)$ in such nuclear matter with $\xi = (N - Z)/A$ is the ratio of the energy-density to the local density, expressed as [26,28,41]

$$
B(\rho, \xi) = 0.3 \left(\frac{\hbar^2}{2M} \right) \left(\frac{3\pi^2}{2} \right)^{2/3}
$$
$$
\times [(1 - \xi)^{5/3} + (1 + \xi)^{5/3}] \rho^{2/3} + \nu(\rho, \xi). \quad (1)
$$

M is the nucleon mass and the mean-field $\nu(\rho, \xi)$ is
$$
\nu(\rho, \xi) = \lambda_1 (1 + a_1 \xi^2) \rho + \lambda_2 (1 + a_2 \xi^2) \rho^{4/3}
$$
$$
+ \lambda_3 (1 + a_3 \xi^2) \rho^{5/3}. \quad (2)
$$

For infinite symmetric nuclear matter (ISNM)
$$
\nu_S(\rho, \xi = 0) = \lambda_1 \rho + \lambda_2 \rho^{4/3} + \lambda_3 \rho^{5/3}. \quad (3)
$$

For application to finite nuclei, the EDF theory has been extended [29] to include the density-gradient correction

TABLE I. Mean-field parameters λ's for different K values, corresponding $J_R/256$ and η, adjusted for the same E_{calc}.

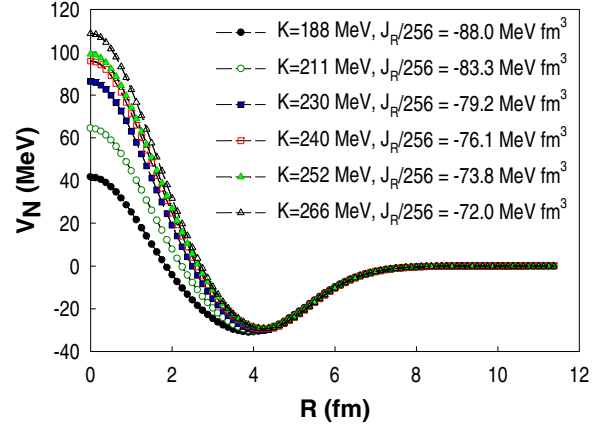| K(MeV)	λ_1	λ_2	λ_3	η	$J_R/256$ (MeV fm^3)
188	-741.28	$+1179.55$	-467.54	8.0	-88.00
211	-709.55	$+1040.18$	-451.07	8.38	-83.32
230	-676.40	$+895.80$	-173.80	8.74	-79.20
240	-696.21	$+953.98$	-214.36	9.05	-76.12
252	-675.34	$+880.19$	-146.81	8.70	-73.81

FIG. 2. (Color online) K dependence of the EDF-generated $^{16}\mathrm{O} - ^{16}\mathrm{O}$ nuclear potential with the volume integral $J_R/256$.

through the inhomogeneity parameter η and the Coulomb terms. After using Eq. (1), this results in the energy of a nucleus as [26,29,41]

$$
E = \int \left[B(\rho, \xi) \rho(\mathbf{r}) + \left(\frac{\hbar^2}{8M} \right) \eta (\nabla \rho)^2 \right] d^3 \mathbf{r}
$$
$$
+ \int \left[\frac{e}{2} \Phi_C(\mathbf{r}) \rho_P - 0.739 e^2 \rho_P^{4/3} \right] d^3 \mathbf{r}. \quad (4)
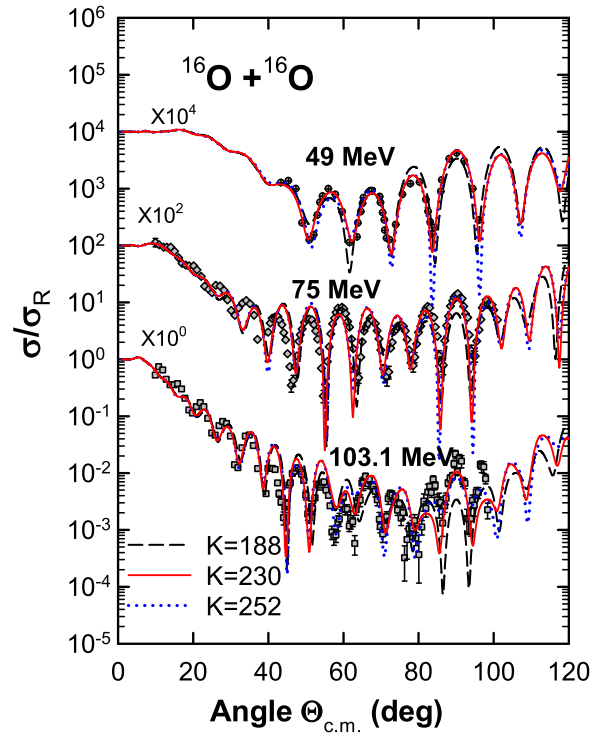$$

FIG. 3. (Color online) OM predictions are compared with the $^{16}\mathrm{O} + ^{16}\mathrm{O}$ elastic scattering data at $E_{\mathrm{lab}} = 49.0, 75.0$, and 103.1 MeV. The relative performances of the EDF-derived potentials for $K = 188$, 230, and 252 MeV are shown to indicate the K dependence on $J_R/256$.

TABLE II. Potential parameters for the ^{16}O + ^{16}O elastic scattering in the energy range 31–350 MeV for $R_C = 5$ fm with $J_R/256$ values and χ^2 for the fits. The depths are in MeV; geometry parameters in fm; and $J_R/(256)$ in MeV fm^3.

E_{lab}	V_0	R_0	a_0	V_1	R_1	D_1	$J_R/256$	χ^2
31.0	29.9	5.735	0.653	50.0	2.84	0.0	−79.2	0.29
41.0	31.2	5.652	0.742	103.0	2.34	0.0	−79.1	1.80
49.0	76.0	5.418	0.864	158.0	3.662	0.0	−78.7	1.60
59.0	95.0	5.216	0.785	228.0	2.30	1.360	−77.8	7.90
75.0	79.0	5.800	0.575	107.0	2.11	2.827	−76.3	3.60
80.6	100.0	6.170	0.544	107.5	3.586	2.325	−75.6	5.10
87.2	108.0	5.695	0.526	146.0	1.633	3.480	−75.0	6.20
92.4	37.4	6.526	0.385	104.0	0.715	3.936	−74.0	7.70
94.8	45.6	6.150	0.505	102.0	0.835	3.83	−73.7	6.00
98.6	87.0	5.820	0.550	162.0	1.372	3.326	−73.2	4.70
103.1	49.0	6.050	0.520	141.0	0.595	4.00	−72.4	6.50
115.9	105.0	6.090	0.480	123.0	1.924	3.838	−70.5	8.20
124.0	83.0	5.292	0.660	130.0	0.800	4.208	−69.0	18.8
145.0	79.0	4.964	0.790	353.0	0.290	3.855	−64.9	5.50
250.0	180.0	5.040	0.673	170.0	1.700	3.860	−32.5	18.4
350.0	151.0	5.040	0.670	162.0	1.783	3.742	+20.3	3.20

TABLE III. Same as Table II for the imaginary part of the potential with associated volume integral per nucleon pair $J_I/256$.

E_{lab}	W_S	D_S	R_S	W_0	R_W	$J_I/256$	χ^2
31.0	2.00	8.10	0.13	20.0	3.2	−15.8	0.29
41.0	3.00	7.48	0.11	29.0	3.2	−22.3	1.80
49.0	2.30	7.20	0.50	32.7	3.2	−28.5	1.60
59.0	2.60	7.96	0.21	46.0	3.4	−42.3	7.90
75.0	1.80	7.11	0.15	86.0	3.40	−70.5	3.60
80.6	1.25	8.00	0.82	90.0	3.40	−82.7	5.10
87.2	0.44	8.37	0.40	137.0	3.40	−118.2	6.20
92.4	0.40	8.95	0.30	187.0	3.40	−160.7	7.70
94.8	0.33	8.44	0.77	200.0	3.35	−165.2	6.00
98.6	1.20	6.61	0.28	217.0	3.30	−170.9	4.70
103.1	0.34	8.94	0.15	255.0	3.35	−208.9	6.50
115.9	1.30	6.40	0.10	260.0	3.35	−213.1	8.20
124.0	0.30	7.89	0.10	360.0	3.28	−276.5	18.8
145.0	0.50	7.14	0.11	413.0	3.14	−278.4	5.50
250.0	0.25	6.73	0.13	1080.0	3.00	−634.5	18.4
350.0	0.35	6.56	0.32	1258.0	2.98	−724.6	3.20

The last integral is from Coulomb terms. For a given separation R, the potential $V(R)$ between the interacting nuclei is given by

$$V(R) = E[\rho(\mathbf{r}, R)] - E[\rho_1(\mathbf{r}, R = \infty)] - E[\rho_2(\mathbf{r}, R = \infty)], \tag{5}$$

with subscripts referring to the composite system and the two interacting nuclei. The density distribution of the composite system is calculated in the sudden approximation, i.e., as a simple sum of the density distributions. Further details on the derivation of the nucleus-nucleus potential are given in [26,30,42].

B. K-dependence of ^{16}O-^{16}O nuclear potential

Figure 1 shows EOS of BCD [28] corresponding to $K \approx 188$ MeV [27,43]. Harder EOSs for higher K's with identical features at lower densities up to saturation have been simulated in the figure with

$$K = 9\rho_0^2 \left[\frac{d^2(E/A)}{d\rho^2} \right]_{\rho = \rho_0} \tag{6}$$

at the saturation point with $\rho(r) = \rho_0$. The associated mean-fields, derived from them, are listed in Table I.

Starting first with the mean-field corresponding to $K = 188$ MeV and $\eta = 8.0$ [41], we performed the EDF calculations using $c = 2.512$, $z = 0.45$ fm, and the normalization $\rho_0 = 0.181$ fm^{-3} [39] in $\rho(r) = \rho_0[1 + \exp(\frac{r-c}{z})]^{-1}$, the DDF of ^{16}O. The EDF calculation produced the binding energy, $E_{\text{calc}} = 129.6$ MeV compared to the experimental value 127.6 MeV [44] of ^{16}O. For other mean-fields, only the η value in Eq. (4) is adjusted for the same E_{calc}. The values of η and volume integral per nucleon pair $J_R/256$ of the EDF-generated nuclear potentials for different K values are noted in Table I with the potentials plotted in Fig. 2.

III. ANALYSIS AND RESULTS

A. Optical Model analysis

The OM analyses have been carried out using the code SFRESCO, which incorporates the coupled-channels code FRESCO2.5 [45] and the χ^2-minimization code MINUIT [46]. The experimental data are taken from [2,47,48]. The data are converted from the ratios to the Mott cross section to those normalized to Rutherford scattering. The following points are considered:

(a) BCD's EOS is based on DDFs and the Pauli effect for nuclear ground states and hence the EDF theory based on it produces NM potentials valid for *zero* excitation energy (E_x) of the composite nucleus. Thus, we do not expect excellent fits to the data at nonzero E_x corresponding to higher projectile energies using the EDF-generated NM potentials without further tuning.

(b) The continuous and discrete ambiguities in the OM potentials can be minimized by selecting sets that fit the data with single digit χ^2. The latter can be removed by plotting $J_R/256$ vs E_x (or E_{lab} [26]) to ensure that all sets belong to the same potential family [49].

(c) The study of K sensitivity to experimental data can be realized by analyzing them with OM potentials of known K values.

B. Parametrization of the OM potential

The nuclear potential for separation R, $V_N(R)$ is parametrized with the following analytic expression:

$$V_N(R) = -V_0 \left[1 + \exp\left(\frac{R - R_0}{a_0} \right) \right]^{-1}$$

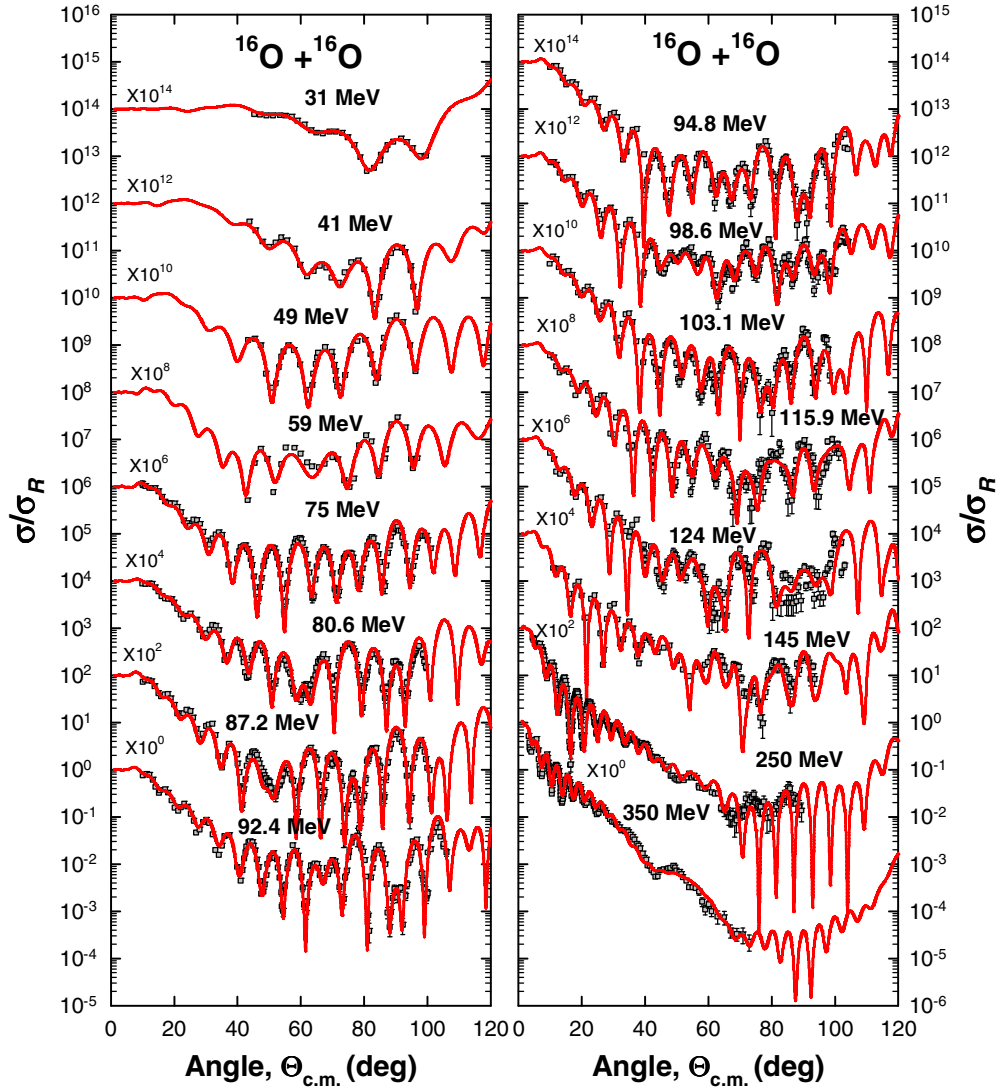$$+ V_1 \exp\left[-\left(\frac{R - D_1}{R_1} \right)^2 \right] \tag{7}$$

FIG. 4. (Color online) Same as Fig. 3 for the best fits at 16 energies obtained by an empirical adjustment of the OM parameters including those for the real part of the potentials.

and the Coulomb potential $V_C(R)$ is that for a uniformly charged sphere of radius $R_C = 5$ fm. The imaginary part of the OM potential is taken phenomenologically as

$$W(R) = -W_0 \exp\left[-\left(\frac{R}{R_W}\right)^2\right]$$
$$- W_S \exp\left[-\left(\frac{R - D_S}{R_S}\right)^2\right]. \quad (8)$$

C. Examination of K-sensitivity of EDF-derived potential

To examine the K sensitivity, the data for 49.0, 75.0, and 103.1 MeV have been fitted with the EDF-derived real potentials left unchanged for individual K values and empirically adjusted imaginary potential parameters. Consideration of the relative χ^2 from the NM potentials for $K = 188$, 230, and 252 MeV at each of the energies and visual inspection on the fits in Fig. 3 suggest that the data at the three energies are

best described by the EDF-derived potential for $K = 230$ MeV. Thus, K dependence of the elastic scattering data is indicated, although the fits to data are not impressive, just because the EDF calculation from BCD without energy-dependence built into it is valid for $E_x = 0.0$ of the composite nucleus.

D. Deduction of the value of K

In the next step, we have analyzed the experimental data at 16 points in the energy interval 31–350 MeV. The path to the determination of a value for K is as follows:

(a) The parameters of the potential are further tuned to obtain high-quality fits to the experimental data. The volume integrals $J_R/256$ are calculated. Although the OM potential parameters are scattered as a result of global searches for the χ^2 of single digits, they are consistent in volume integrals (see Tables II and III). The fits are displayed in Fig. 4.
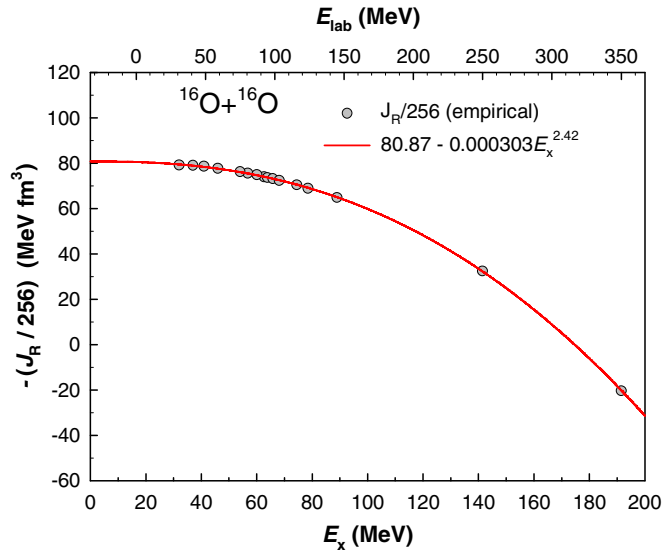
FIG. 5. (Color online) Variation of $J_R/256$ with E_x and the regression curves through the derived points in open circles.

(b) These values of $J_R/256$ are plotted vs E_x, with $E_x = 16.5 + E_{lab}/2$, where all the points end up on a smooth curve ensuring the same potential family [49].

(c) The energy variation of $J_R/256$ is regressed by a power function $80.9 - 0.0003E_x^{2.42}$ (Fig. 5). The intercept term is very well determined, leading to the value $J_R/256(E_x = 0) = 80.9 \pm 1.1 \, \text{MeV fm}^3$. The total error-bar includes the uncertainties from the individual $J_R/256$ values, curve-fitting, and extrapolation.

(d) Finally Table I is used to estimate the nuclear matter incompressibility from the extrapolated value of $J_R/256$ at $E_x = 0$ considering the linearity between the successive values of K and $J_R/256$. This leads to $K = 222 \pm 5 \, \text{MeV}$.

For $E_x = 0$ the volume integrals of the potentials used to fit the data should agree with the EDF potentials of the same volume integral in the surface region responsible for elastic scattering at low energies. We checked and found this to be true for the real potentials fitting the 31 and 41 MeV data and the EDF potential for $K = 230 \, \text{MeV}$.

Thus instead of an excursion from the EDF calculations to the data-fitting, we have opted for a reverse path from fitting the data to the EDF calculations, through a comparison of volume integral $J_R/256$ of the best fitting by the empirical

potential parameters with the EDF-derived values. This leads to significantly better fits as well as a more precise estimate of K. It would be interesting to see if this value can be confirmed in a repeat analysis on a similar system, e.g., ^{40}Ca $- ^{40}$Ca. The impressive results from our simple method may be improved by an extended BCD theory with energy dependence built into it, as suggested by [50,51].

IV. CONCLUSIONS

The study concerns the first application of the NM potentials with microscopically built repulsive core, based on the EOS of BCD for ISNM, to examine the K sensitivity on the elastic scattering. BCD's EOS involves a mean-field which is the non-Coulomb potential in nucleonic matter. The field is calculated using the Pauli-exchanged K matrices [28] of a realistic NN potential of [52] which describes all the deuteron properties and two-nucleon scattering up to the pion-production energy. The excellent description of the data with NM potentials calls for a reanalysis of the issue of deep vs shallow OM potentials. A careful examination of S-matrix elements and model-independent studies such as [53] may shed more light on the issue. Table II shows that the NM potential changes smoothly from overall attractive (negative) $J_R/256$ values to a repulsive (positive) one at high energies in line with observations on heavy- [9,54] and light-ion [55–58] systems.

The calibration curve, $J_R/256$ vs E_x, in Fig. 5, is based on the empirical NM potentials giving the profound descriptions to the elastic scattering data. The deduced result $K = 222 \pm 5 \, \text{MeV}$, corresponding to the extrapolated $J_R/256$ at $E_x = 0.0 \, \text{MeV}$ in Fig. 5, agrees closely with the empirical values obtained in [12–14]. The intriguing aspect of BCD's EDF is that its underlying theory applies appropriately the Pauli principle to the EOS of ISNM. Hence its simple theory, without requiring the transformation from K_A to K which entails a large uncertainty in the deduced value of K [3,16–18,25], yields directly the K value for infinite cold nuclear matter.

[1] D. T. Khoa, W. von Oertzen, H. G. Bohlen, G. Bartnitzky, H. Clement, Y. Sugiyama, B. Gebauer, A. N. Ostrowski, Th. Wilpert, M. Wilpert, and C. Langner, Phys. Rev. Lett. **74**, 34 (1995); D. T. Khoa and W. von Oertzen, Phys. Lett. B **342**, 6 (1995).

[2] D. T. Khoa *et al.*, J. Phys. G **34**, R111 (2007).

[3] J. M. Pearson, Phys. Lett. B **271**, 12 (1991).

[4] M. E. Brandan and G. R. Satchler, Phys. Rep. **285**, 143 (1997).

[5] K. Rusek *et al.*, Nucl. Phys. A **407**, 208 (1983).

[6] G. Tungate *et al.*, Phys. Lett. B **98**, 347 (1981).

[7] V. Yu. Denisov and O. I. Davidovskaya, Phys. At. Nucl. **73**, 404 (2010).

[8] V. Yu. Denisov and V. A. Nesterov, Phys. At. Nucl. **73**, 1142 (2010).

[9] T. Furumoto, Y. Sakuragi, and Y. Yamamoto, Phys. Rev. C **82**, 044612 (2010); **82**, 029908(E) (2010).

[10] T. Furumoto, Y. Sakuragi, and Y. Yamamoto, Phys. Rev. C **80**, 044614 (2009).

[11] T. Furumoto, Y. Sakuragi, and Y. Yamamoto, Phys. Rev. C **79**, 011601(R) (2009).

[12] Ş. Mişicu and H. Esbensen, Phys. Rev. Lett. **96**, 112701 (2006).

[13] Ş. Mişicu and H. Esbensen, Phys. Rev. C **75**, 034606 (2007).

[14] H. Esbensen, Phys. Rev. C **77**, 054608 (2008).

[15] O. N. Ghodsi and V. Zanganeh, Nucl. Phys. A **846**, 40 (2010).

[16] J.-P. Blaizot *et al.*, Nucl. Phys. A **591**, 435 (1995).

[17] J.-P. Blaizot, Nucl. Phys. A **649**, 61c (1999).

[18] T. Li *et al.*, Phys. Rev. C **81**, 034309 (2010).

[19] D. H. Youngblood, C. M. Rozsa, J. M. Moss, D. R. Brown, and J. D. Bronson, Phys. Rev. Lett. **39**, 1188 (1977).

[20] D. H. Youngblood *et al.*, Nucl. Phys. A **649**, 49c (1999).

[21] D. H. Youngblood, Y. W. Lui, and H. L. Clark, Phys. Rev. C **55**, 2811 (1997).

[22] D. H. Youngblood, H. L. Clark, and Y. W. Lui, Phys. Rev. C **57**, 1134 (1998).

[23] E. Khan, N. Paar, D. Vretenar, Li-Gang Cao, H. Sagawa, and G. Coló, Phys. Rev. C **87**, 064311 (2013).

[24] J. R. Stone, N. J. Stone, and S. A. Moszkowski, Phys. Rev. C **89**, 044316 (2014).

[25] G. Coló, N. V. Giai, J. Meyer, K. Bennaceur, and P. Bonche, Phys. Rev. C **70**, 024307 (2004).

[26] S. Hossain *et al.*, J. Phys. G **40**, 105109 (2013).

[27] A. K. Basak *et al.*, Europhys. Lett. **94**, 62002 (2011).

[28] K. A. Brueckner, S. A. Coon, and J. Dabrowski, Phys. Rev. **168**, 1184 (1968).

[29] K. A. Brueckner *et al.*, Phys. Rev. **171**, 1188 (1968); **181**, 1543 (1969).

[30] K. A. Brueckner, J. R. Buchler, and M. M. Kelly, Phys. Rev. **173**, 944 (1968).

[31] I. Reichstein and F. B. Malik, Phys. Lett. B **37**, 344 (1971).

[32] C. Ngô *et al.*, Nucl. Phys. A **252**, 237 (1975).

[33] S. K. Das *et al.*, Phys. Rev. C **60**, 044617 (1999).

[34] S. K. Das *et al.*, Phys. Rev. C **62**, 054605 (2000).

[35] S. K. Das *et al.*, Phys. Rev. C **64**, 034605 (2001).

[36] S. K. Das *et al.*, Phys. Rev. C **62**, 054606 (2000).

[37] V. B. Soubbotin, W. von Oertzen, X. Vinas, K. A. Gridnev, and H. G. Bohlen, Phys. Rev. C **64**, 014601 (2001).

[38] D. Baye, Phys. Rev. Lett. **58**, 2738 (1987).

[39] A. K. Chaudhuri and B. Sinha, Nucl. Phys. A **455**, 169 (1986).

[40] F. Michel, G. Reidemeister, and S. Ohkubo, Phys. Rev. C **63**, 034620 (2001).

[41] M. A. Hooshyar, I. Reichstein, and F. B. Malik, *Nuclear Fission and Cluster Radioactivity* (Springer, Berlin, 2005).

[42] S. Hossain *et al.*, Eur. Phys. J. A **41**, 215 (2009).

[43] A. V. Pozdnyakov, I. Reichstein, Z. F. Shehadeh, and F. B. Malik, Cond. Matter Theories **10**, 365 (1995).

[44] A. H. Wapstra and G. Audi, Nucl. Phys. A **432**, 1 (1985).

[45] I. J. Thompson, Comp. Phys. Rep. **7**, 167 (1988).

[46] F. James and M. Roos, Comput. Phys. Commun. **10**, 343 (1975).

[47] M. P. Nicoli *et al.*, Phys. Rev. C **60**, 064608 (1999).

[48] J. V. Maher *et al.*, Phys. Rev. **188**, 1665 (1969); Y. Sugiyama *et al.*, Phys. Lett. B **312**, 35 (1993); Y. Kondo *et al.*, *ibid.* **365**, 17 (1996).

[49] P. Mohr *et al.*, Phys. Rev. C **82**, 044606 (2010).

[50] B. Behera, K. C. Panda, and R. K. Satpathy, Phys. Rev. C **22**, 148 (1980).

[51] D. M. Brink and Fl. Stancu, Nucl. Phys. A **243**, 175 (1975).

[52] K. A. Brueckner and J. L. Gammel, Phys. Rev. **109**, 1023 (1958).

[53] G. Bartnitzky *et al.*, Phys. Lett. B **365**, 23 (1996).

[54] T. Furumoto *et al.*, J. Phys.: Conf. Series **381**, 012092 (2012).

[55] J. S. Al-Khalili, J. A. Tostevin, and R. C. Johnson, Phys. Rev. C **41**, R806(R) (1990).

[56] V. K. Mishra, S. Hama, B. C. Clark, R. E. Kozack, R. L. Mercer, and L. Ray, Phys. Rev. C **43**, 801 (1991).

[57] N. van Sen *et al.*, Phys. Lett. B **156**, 185 (1985).

[58] N. van Sen *et al.*, Nucl. Phys. A **464**, 717 (1987).